

Copyright (2011) American Institute of Physics. This article may be downloaded for personal use only. Any other use requires prior permission of the author and the American Institute of Physics.

The following article appeared in (**J. Chem. Phys.**, **141**, 18C531, **2014**) and may be found at (<http://scitation.aip.org/content/aip/journal/jcp/141/18/10.1063/1.4898366>).

The role of material flexibility on the drying transition of water between hydrophobic objects: A thermodynamic analysis

Y. Elia Altabet and Pablo G. Debenedetti

Citation: *The Journal of Chemical Physics* **141**, 18C531 (2014); doi: 10.1063/1.4898366

View online: <http://dx.doi.org/10.1063/1.4898366>

View Table of Contents: <http://scitation.aip.org/content/aip/journal/jcp/141/18?ver=pdfcov>

Published by the [AIP Publishing](#)

Articles you may be interested in

Publisher's Note: "The role of material flexibility on the drying transition of water between hydrophobic objects: A thermodynamic analysis" [*J. Chem. Phys.* **141**, 18C531 (2014)]

J. Chem. Phys. **141**, 189901 (2014); 10.1063/1.4901427

Self-assembly of metal nanorod arrays into hierarchical clusters and evolution of their hydrophobic behaviour
AIP Conf. Proc. **1536**, 193 (2013); 10.1063/1.4810166

A computational investigation of the phase behavior and capillary sublimation of water confined between nanoscale hydrophobic plates

J. Chem. Phys. **137**, 144501 (2012); 10.1063/1.4755750

Water droplets on a hydrophobic insulator surface under high voltages: A thermal perspective

Appl. Phys. Lett. **101**, 131602 (2012); 10.1063/1.4754689

Observation of hydrophobic-like behavior in geometrically patterned hydrophilic microchannels

Biomicrofluidics **4**, 044103 (2010); 10.1063/1.3499416



The role of material flexibility on the drying transition of water between hydrophobic objects: A thermodynamic analysis

Y. Elia Altabet and Pablo G. Debenedetti^{a)}

Department of Chemical and Biological Engineering, Princeton University, Princeton, New Jersey 08544, USA

(Received 15 August 2014; accepted 4 October 2014; published online 22 October 2014; publisher error corrected 28 October 2014)

Liquid water confined between hydrophobic objects of sufficient size becomes metastable with respect to its vapor at separations smaller than a critical drying distance. Macroscopic thermodynamic arguments predicting this distance have been restricted to the limit of perfectly rigid confining materials. However, no material is perfectly rigid and it is of interest to account for this fact in the thermodynamic analysis. We present a theory that combines the current macroscopic theory with the thermodynamics of elasticity to derive an expression for the critical drying distance for liquids confined between flexible materials. The resulting expression is the sum of the well-known drying distance for perfectly rigid confining materials and a new term that accounts for flexibility. Thermodynamic arguments show that this new term is necessarily positive, meaning that flexibility increases the critical drying distance. To study the expected magnitude and scaling behavior of the flexible term, we consider the specific case of water and present an example of drying between thin square elastic plates that are simply supported along two opposite edges and free at the remaining two. We find that the flexible term can be the same order of magnitude or greater than the rigid solution for materials of biological interest at ambient conditions. In addition, we find that when the rigid solution scales with the characteristic size of the immersed objects, the flexible term is independent of size and vice versa. Thus, the scaling behavior of the overall drying distance will depend on the relative weights of the rigid and flexible contributions. © 2014 AIP Publishing LLC. [<http://dx.doi.org/10.1063/1.4898366>]

I. INTRODUCTION

Fluids under spatial confinement can exhibit remarkably different behavior than their bulk counterparts, and while this has been appreciated for some time,¹ the scientific and technological implications of this phenomenon remain an active subject of investigation. Aqueous solutions under confinement have been the object of particularly intense interest, due in part to water's intimate connection to the existence of life on Earth² and the unique scrutiny it has received as a bulk fluid.^{3,4} Recent studies of aqueous systems under confinement include characterizing the transport of water through carbon nanotubes,⁵ modifying reaction equilibria under mesoscale confinement,⁶ and observing large salinity-driven currents across boron-nitride nanotubes.⁷ In addition to providing a rich platform for inquiries of basic scientific interest, the behavior of water in confined geometries is crucial to the design of numerous technologies, including membranes for desalination,⁸ dip-pen nanolithography,⁹ and microfluidic arrays for biological assays.¹⁰

The stability of water under hydrophobic confinement has attracted considerable attention^{11–13} by serving as a basic model for fundamental studies of the hydrophobic effect and its relation to the aggregation behavior of hydrophobic objects. The hydrophobic effect plays a pivotal role in the formation and function of molecular assemblies such

as micelles,^{14,15} globular proteins,¹⁶ lipid membranes,¹⁷ and membrane channels.^{18–20} In 1959, Kauzmann²¹ first proposed the connection between the tendency for oil and water to segregate and the stability of globular proteins, a view that has now reached a broad consensus.²² While the importance of hydrophobic interactions may be well established, quantifying the many features of this rich phenomenon to the point of attaining a comprehensive understanding remains an active pursuit.²³ Such an understanding is certainly required for the rational design of proteins and other macromolecular assemblies.

An important advance in developing an understanding of the hydrophobic effect was identifying the difference between the hydration of small and large apolar solutes, which ultimately dictates their tendency to aggregate in solution.²³ Small hydrophobes can incorporate into water's hydrogen bond network at the cost of limiting the solvent's degrees of freedom, resulting in a free energy of solvation that is dominated by a negative entropic contribution and scales with the particle's volume. This solvation behavior is reflected in the ability of theories based on the work of cavity creation,²⁴ cavity distribution²⁵ or related information-based approaches^{26–28} to successfully describe the solvation behavior of small apolar solutes. Near large hydrophobes, roughly 1 nm in size at ambient conditions, water is unable to maintain the same number of hydrogen bonds as the bulk fluid. Breaking such bonds results in solvation free energies dominated by an enthalpic penalty that can be macroscopically characterized through the surface tension of the solute/water

^{a)} Author to whom correspondence should be addressed. Electronic mail: pdebene@princeton.edu

interface. That the solvation behavior of large apolar solutes is characterized by interfacial energetics was first predicted theoretically by Stillinger²⁹ and characterized in molecular dynamics simulations by Lee, McCammon and Rossky.³⁰ This crossover from small to large solute hydration behavior has been incorporated into a unified theory by Lum, Chandler, and Weeks³¹ and subsequent studies have explored how this crossover length can be manipulated.^{32,33}

The different hydration behavior of small and large apolar solutes has direct bearing on the stability of water confined between such solutes and the latter's tendency to aggregate. Small solute pairs with weak intermolecular interactions are not favored to aggregate, and separation by a single water molecule is often the most stable conformation.³⁴⁻³⁶ Large apolar solute pairs are strongly favored to aggregate due to the resulting reduction in solvent accessible surface area.^{23,37} This drive towards aggregation is reflected in the stability of the confined liquid film. As two large apolar solutes are brought together, at small enough separations, the confined liquid becomes metastable with respect to its vapor. The separation below which the liquid becomes metastable is often referred to as the critical drying distance. Drying or cavitation to a vapor phase results in a strong attractive force that can promote the aggregation of the confining objects.^{12,31} Surface-induced drying transitions have been observed and characterized in numerous simulations of idealized³⁷⁻⁴⁹ and biologically relevant systems^{18-20,50-54} and have also been invoked to interpret the long-range hydrophobic attraction.⁵⁵⁻⁶⁰

Macroscopic thermodynamic arguments can predict this drying transition, and the model system often invoked is that of two rigid parallel $L \times L$ plate-like solutes, separated by a distance D , and immersed in a bath of water at a fixed chemical potential μ and temperature T .^{43,61} We consider the control volume to be a $L \times L \times (D + \varepsilon)$ rectangular box, where ε is an arbitrarily small length that allows inclusion of the interface between the plates and the surrounding bulk fluid yet excludes any bulk fluid itself. The free energy (grand potential) of the confined liquid is given by

$$\Omega_l = -p_l L^2 D + 4\gamma_{ls} L^2, \quad (1)$$

and, if we treat the vapor/liquid interface as flat, the free energy of the corresponding vapor is given by

$$\Omega_v = -p_v L^2 D + 2\gamma_{vs} L^2 + 2\gamma_{ls} L^2 + 4\gamma_{vl} L D, \quad (2)$$

where p_l and p_v are the pressure of the liquid and vapor, and γ_{ls} , γ_{vs} , and γ_{vl} are the liquid/solid, vapor/solid, and vapor/liquid interfacial tensions, respectively. Equating the above free energies and solving for D yields the separation below which the confined liquid is metastable with respect to its vapor,³⁸

$$D_c = -\frac{2\gamma_{vl} \cos \theta}{(p_l - p_v) \left[1 + \frac{4\gamma_{vl}}{L(p_l - p_v)} \right]} = -\frac{2\gamma_{vl} \cos \theta}{\Delta p [1 + \phi]}, \quad (3)$$

where $\Delta p = p_l - p_v$, $\phi = \frac{4\gamma_{vl}}{L\Delta p}$, and Young's equation⁶² relates the two fluid/solid interfacial tensions to γ_{vl} and the contact angle θ . On a sufficiently soft material, the contact angle of a droplet is not well-described by Young's equation due to deformations induced by the vertical component of surface

tension.⁶³⁻⁶⁵ For consistency between this discussion and our subsequent analysis, we consider θ to be the contact angle one would observe if the material were perfectly rigid. In other words, θ is a proxy for the chemical composition of the material, not its mechanical properties.

The dimensionless group ϕ can be interpreted as the ratio of the two free energies that oppose drying: the formation of a vapor/liquid interface and the increase in the bulk free energy of the confined fluid. For $\phi \ll 1$, the increase of bulk free energy provides the main barrier to drying and the critical drying distance becomes independent of the size of the plates.

$$D_c = -\frac{2\gamma_{vl} \cos \theta}{\Delta p}. \quad (4)$$

For $\phi \gg 1$, the formation of an interface provides the main barrier to drying and the critical drying distance is proportional to the characteristic size of the plates.

$$D_c = -\frac{L \cos \theta}{2}. \quad (5)$$

Even though these arguments are strictly valid in the thermodynamic limit, recent simulations have found the $\phi \gg 1$ limit to be roughly quantitative for nanoscale solutes in water,^{46,66} and a recent Monte Carlo study of these arguments applied to a 2D Lennard-Jones fluid has found quantitative agreement over a wide span of ϕ .⁶⁷ In addition, evaporation of a water-like fluid under hydrophobic confinement was first predicted by statistical mechanical arguments in Ref. 68.

While the principles summarized above may inform our intuition on the behavior of ideal apolar solutes, real materials of interest are often chemically and topographically heterogeneous. This fact has motivated a number of studies on systems with less idealized features, with several major themes emerging. Studies of the hydrophobic response of chemically heterogeneous materials find that relatively few attractive regions on a predominantly hydrophobic surface can produce both a considerable change in the structure of the interfacial water next to free surfaces^{69,70} and suppress complete drying under confinement.^{53,71-74} Chemical heterogeneity seems to strongly affect the kinetics of evaporation as well.^{39,40} Investigations on the role of topography suggest that a local feature that cannot be incorporated into water's hydrogen bond network will result in large-solute type hydration^{75,76} and promote a drying transition under confinement.^{50,53,77} While a number of avenues within this theme of heterogeneity remain to be explored,¹³ even less attention has been paid to the manner in which the mechanical properties of the confining material may alter the phase behavior of confined water.

Several simulation studies have explored how flexibility alters the drying behavior of water under hydrophobic confinement. Beckstein and Sansom⁷⁸ studied the role of flexibility on water permeation through a pore representative of a membrane channel. By varying the harmonic spring constant of each pore atom, the authors found that increasing flexibility shifted the equilibrium water content of the pore towards the vapor state. Andreev, Reichman, and Hummer⁷⁹ explored the effect of flexibility on the internal hydration of carbon nanotubes and found that more flexible nanotubes promoted drying and impeded water transport relative to what has

been found for rigid nanotubes.⁸⁰ Xu and Molinero⁶⁶ studied the vapor-liquid oscillations between hydrophobic disks and found that introducing a modest spring constant acting on each disk atom had a negligible effect on the drying behavior. To the best of our knowledge, no theory has been presented in the literature.

In this paper, we present a theory that blends the current macroscopic theory reviewed above with the thermodynamics of elasticity to derive the critical drying distance for a fluid confined between flexible materials. The resulting expression for the critical drying distance is the sum of the expression for perfectly rigid solutes and a term associated with the elastic response of the material. Thermodynamic arguments show that this elastic term is necessarily positive, meaning that flexibility promotes drying, resulting in an increase in the critical drying distance. We then consider a specific example of drying of water between simply supported plates with two free edges in order to estimate the magnitude of the flexible term and its scaling behavior with respect to plate size. We show that the elastic term can be of the same order of magnitude or greater than the rigid term for Young's moduli within the range of biologically relevant materials such as amyloid fibrils. Like the perfectly rigid solution, the scaling behavior of the flexible term is controlled by the value of ϕ . However, in the limit $\phi \gg 1$ where the rigid term behaves like a constant for given set of environmental conditions (see Eq. (4)), the flexible term scales with the characteristic size of the solute for a given solute shape and stiffness. For $\phi \ll 1$, on the other hand, while the rigid term scales linearly with solute size (see Eq. (5)), the flexible term is constant for a given solute shape and stiffness. The different behavior of the rigid and flexible contributions to the overall drying distance suggests that accounting for flexibility may allow considerable versatility in the design of hydrophobic assemblies.

We adopt the following organization in this work. In Sec. II, we derive an expression for the critical drying distance between linear elastic plates. In Sec. III, we apply the general framework to the particular case of plates that are simply supported along two opposite edges and free at the re-

maining two. Section IV contains a discussion of the physical implications of the expressions derived in Secs. II and III. In Sec. V, we summarize the conclusions of this study and suggest additional lines of inquiry that build upon this work.

II. CRITICAL DRYING DISTANCE BETWEEN FLEXIBLE PLATES

In this section, we develop an expression for the critical drying distance between flexible plates by merging the thermodynamics of elasticity with the model reviewed in the Introduction. Recall that upon evaporation, there exists a pressure difference across the plates as well as a vapor/liquid interface, which if the plates are unrestrained, ultimately act as forces that promote aggregation. If the plates are restrained against net translation, both the pressure difference across the plates and the vapor/liquid interface that terminates at the edge of the plates can act as loads that induce deformation (Figure 1). These forces acting on the plates correspond directly to the energetic penalties associated with drying, and allowing the material to deform under these forces tends to relieve these penalties, at the cost of introducing strain in the plates. The interplay between relieving the penalties due to drying and the added energetic penalty of straining the plates is the crux of this thermodynamic analysis.

By accounting for the thermodynamic contribution of deformation to the free energies of the wet and dry states, we can develop an expression for the critical drying distance in a manner akin to the expression for perfectly rigid plates. In this model, there are no unbalanced forces acting on the unstrained plates with confined liquid, so flexibility does not introduce any changes into the free energy of the confined liquid. In presenting this picture of the wet state (as well as the subsequent dry state), we have assumed that any deformations due to fluid/solid interfacial tensions are negligible, as the rigidity (defined in Sec. III) associated with loading normal to the plate is much smaller than the rigidity associated with in-plane loading. Thus, the expression for Ω_l remains unchanged and is given by Eq. (1).

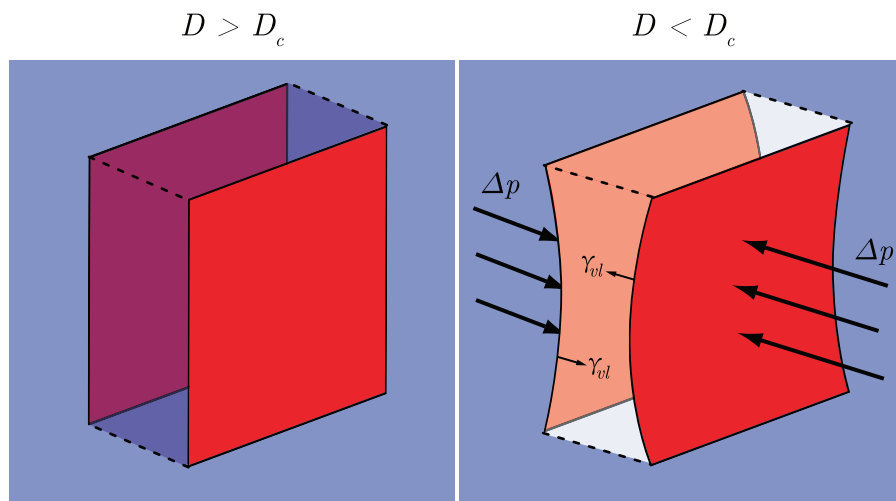


FIG. 1. Schematic of wet ($D > D_c$) and dry ($D < D_c$) states of water between flexible plates. In the wet state, there are no imbalanced forces. In the dry state, the pressure difference (Δp) and vapor/liquid interfacial tension (γ_{vl}) act as forces that induce deformation.

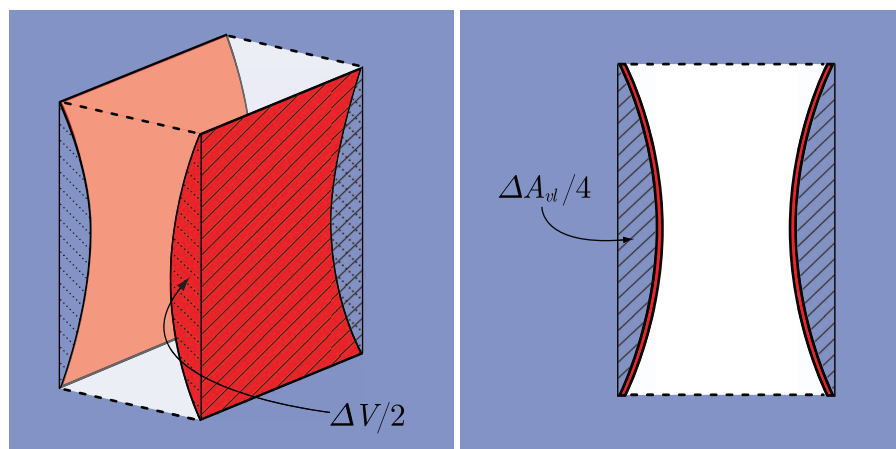


FIG. 2. Deformation that occurs upon drying results in a reduction in both the volume available to the confined vapor (left panel) and the area of the vapor/liquid interface (right panel).

Upon drying, the pressure difference and the force due to vapor/liquid surface tension induce a deformation in the plates, which changes the interfacial areas as well as the volume of the confined region, as illustrated in Figures 1 and 2. Thus, deformation introduces three new terms into the free energy of the vapor state corresponding to the change in volume, change in interfacial area, and strain energy due to deformation (see also Appendix A). By limiting our analysis to small deformations, we can regard the changes in fluid/solid interfacial area as well as curvature effects on the interfacial properties as negligible.

Letting $-\Delta V$ be the decrease in volume available to the confined fluid on account of plate deformation, $-\Delta A_{vl}$ be the corresponding decrease in vapor/liquid interfacial area, and U_{strain} be the total strain energy introduced upon deformation, the free energy of the vapor state can be written as

$$\Omega_v = -p_v L^2 D + 2\gamma_{vs} L^2 + 2\gamma_{ls} L^2 + 4\gamma_{vl} L D - \Delta p \Delta V - \gamma_{vl} \Delta A_{vl} + U_{strain}, \quad (6)$$

where D is the distance between the unstrained plates.

The modification to the free energy of the vapor state (i.e., $-\Delta p \Delta V - \gamma_{vl} \Delta A_{vl} + U_{strain}$) represents the total free energy change associated with going from a state with confined vapor and unstrained plates to a state with confined vapor and strained plates, both at the same temperature. Since material deformation under load is a spontaneous process, we anticipate that this modification accounting for the free energy change associated with deformation is negative, suggesting that flexibility stabilizes the vapor state with respect to its liquid. This will be demonstrated rigorously below (see also Appendix A).

Equating the expressions for Ω_l [Eq. (1)] and Ω_v [Eq. (6)] and solving for D yields the critical drying distance,

$$D_c = -\frac{2\gamma_{vl} \cos \theta}{\Delta p [1 + \phi]} + \frac{\Delta p \Delta V + \gamma_{vl} \Delta A_{vl} - U_{strain}}{L^2 \Delta p [1 + \phi]}, \quad (7)$$

which is simply the sum of the term corresponding to rigid plates and a term associated with flexibility. The term $\Delta p \Delta V + \gamma_{vl} \Delta A_{vl}$ is the work done by the bulk fluid and the vapor/liquid interface, which is equal to $2U_{strain}$ for a linear

elastic solid^{81,82} (see also Appendix A). Thus, for a linear elastic solid, the above equation can be reduced to

$$D_c = -\frac{2\gamma_{vl} \cos \theta}{\Delta p [1 + \phi]} + \frac{\Delta p \Delta V + \gamma_{vl} \Delta A_{vl}}{2L^2 \Delta p [1 + \phi]}. \quad (8)$$

Since the term on the right is positive ($\Delta p > 0$, $\Delta V > 0$, $\Delta A_{vl} > 0$, $\phi > 0$) the drying distance for flexible plates is larger than that of perfectly rigid plates. In other words, flexibility favors evaporation. A common way of characterizing hydrophobic and hydrophilic materials is via the contact angle. For perfectly rigid materials with contact angles less than 90° , the drying distance is negative, so drying is never thermodynamically favored. However, since the term associated with flexibility is necessarily positive, this equation suggests that drying may be possible between flexible materials typically considered hydrophilic ($\theta < 90^\circ$). It should also be mentioned that Eq. (7) yields an estimate of the drying distance between slightly curved rigid plates if U_{strain} is set to zero. Since the term on the right is positive if the plates are bent inward, curvature itself may also promote evaporation between hydrophilic materials, in agreement with recent observations.⁸³

While thermodynamic arguments suggest that flexibility increases the critical drying distance, we can say little about the significance of this statement without an estimate of the magnitude of the flexible term. Unless the flexible term is comparable in magnitude to the rigid term, the arguments presented here are reduced to an intellectual exercise of little consequence. Thus, in Sec. III, we consider a specific example that allows us to make some estimates of the magnitude and scaling behavior of this flexible term.

III. ILLUSTRATIVE EXAMPLE: THE CASE OF TWO PLATES WITH SIMPLY SUPPORTED OPPOSING EDGES

In order to estimate the effect of material flexibility on the drying transition, we develop an expression for the critical drying distance between two identical flexible plates that are restrained by simply supporting the edges at $y = 0, L$ (see Figure 3). To develop this expression we must solve for the deflection profile $w(x, y)$, and then use the profile to

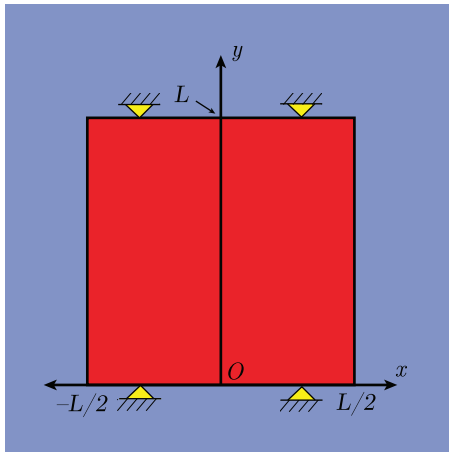


FIG. 3. Schematic of the type of support for the plates in our example. The plate is simply supported at the edges $y = 0, L$, and free to translate at the edges $x = -\frac{L}{2}, \frac{L}{2}$.

develop expressions for the change in volume and interfacial area. Our solution is derived within the context of classical plate theory,⁸⁴ so it is only strictly valid for plates with small thickness-to-length ratios.⁸⁵

A. Plate deflection

The equation of equilibrium for a thin elastic plate subject to an external force Δp is^{81,84}

$$\Delta^2 w(x, y) = \Delta p / D_f, \quad (9)$$

where Δ^2 represents the Laplacian operator applied twice (i.e., $\Delta^2 = \Delta \Delta = (\nabla \cdot \nabla)(\nabla \cdot \nabla)$ where ∇ is the divergence) and D_f is the flexural rigidity of the plates, given by

$$D_f = \frac{Eh^3}{12(1-\nu^2)}, \quad (10)$$

where E is Young's modulus, h is the thickness, and ν is Poisson's ratio (the negative ratio of transverse to axial strain). In this example, we consider the deflection of $L \times L$ plates that are simply supported at the edges $y = 0, L$ and free at the edges $x = -\frac{L}{2}, \frac{L}{2}$ (Figure 3). Choosing the coordinates in this manner ultimately facilitates a more elegant solution. The deflection profile $w(x, y)$ in a given plate is the result of a uniform transverse load Δp acting across the plates due to the pressure difference between the bulk fluid and the confined vapor as well as a force due to the vapor/liquid interfacial tension that pulls on the edge of the plates. Since both plates are identically supported and loaded, we can proceed by solving for $w(x, y)$ for one plate in the positive z -direction and accounting for the second plate in the subsequent analysis.

The boundary conditions at the simply supported edges $y = 0, L$ are no deflections and no bending moments,

$$w = 0 \quad \frac{\partial^2 w}{\partial y^2} + \nu \frac{\partial^2 w}{\partial x^2} = 0. \quad (11a)$$

However, since derivatives of $w(x, y)$ with respect to x vanish along the supported edges, the condition of no bending

moments reduces to

$$\frac{\partial^2 w}{\partial y^2} = 0. \quad (11b)$$

The boundary conditions at edges $x = -\frac{L}{2}, \frac{L}{2}$ are the absence of bending moments and equality between the effective shear force at the edge and the load along the edges,⁸⁴ which in this case is the surface tension.

$$\frac{\partial^2 w}{\partial x^2} + \nu \frac{\partial^2 w}{\partial y^2} = 0, \quad (12a)$$

$$-D_f \left(\frac{\partial^3 w}{\partial x^3} + (2-\nu) \frac{\partial^3 w}{\partial x \partial y^2} \right) = \gamma_{vl}. \quad (12b)$$

Even after assuming a flat vapor/liquid interface, this force should be $\gamma_{vl} \bar{n} \cdot \bar{k}$, where \bar{n} is the unit normal to the plate and \bar{k} is the unit vector in the z -direction. However, since the deflections are small, $\bar{n} \approx \bar{k}$ at any point along the edge, so $\bar{n} \cdot \bar{k} \approx 1$.

Using a series solution of the form proposed by Levy⁸⁴ yields

$$w(x, y) = \frac{\Delta p L^4}{D_f} \sum_{m=1,3,5,\dots}^{\infty} \left[\frac{4}{(m\pi)^5} + A_m \cosh\left(\frac{m\pi x}{L}\right) + B_m \frac{m\pi x}{L} \sinh\left(\frac{m\pi x}{L}\right) \right] \sin\left(\frac{m\pi y}{L}\right), \quad (13)$$

where A_m and B_m are coefficients that depend on ν and ϕ . A more detailed presentation can be found in Appendix B.

The above equation can be collapsed to more tractable expressions by letting the infinite sum evaluated at a point on the plates, which is a dimensionless function of the parameters ϕ and ν , be represented by

$$\tilde{w}(\phi, \nu) = \sum_{m=1,3,5,\dots}^{\infty} \left[\frac{4}{(m\pi)^5} + A_m \cosh(m\pi \tilde{x}) + B_m m\pi \tilde{x} \sinh(m\pi \tilde{x}) \right] \sin(m\pi \tilde{y}), \quad (14)$$

where $\tilde{x} = x/L$ and $\tilde{y} = y/L$. Thus, the general solution can be represented by

$$w(x, y) = \frac{\Delta p L^4}{D_f} \tilde{w}(\phi, \nu). \quad (15a)$$

The deflection is induced by two contributions: the pressure difference across the plates and the vapor/liquid interface at the edges, whose relative weights are embodied in the dimensionless group ϕ . Thus, we see that the two free energies that oppose drying translate into forces acting on the plates upon drying, and the ratio of these forces predicts which one plays a dominant role in inducing deformation. This is apparent if we consider the deformation in the limits of large and small ϕ (see also Appendix B).

When ϕ is large, the surface tension contribution outweighs the bulk pressure term, and the deflection is described by the solution to the case of simply supported plates subject

to a force applied only along the unsupported edges,

$$w(x, y) = \frac{\gamma_{vl} L^3}{D_f} \tilde{w}_s(\nu) \quad \phi \gg 1, \quad (15b)$$

where $\tilde{w}_s(\nu)$ is an infinite sum of similar form as Eq. (14).

When ϕ is small, the deflection is described by the solution to the case of simply supported plates subject to a uniform transverse load Δp .

$$w(x, y) = \frac{\Delta p L^4}{D_f} \tilde{w}_p(\nu) \quad \phi \ll 1. \quad (15c)$$

Note that in both limits, the ϕ -dependence is eliminated.

B. Volume, area, and strain energy

The total change in volume, half of which is illustrated in the left panel of Figure 2, is given by twice the integral over the entire domain of a single plate,

$$\begin{aligned} \Delta V &= 2 \frac{\Delta p L^4}{D_f} \int_{0-\frac{L}{2}}^L \int_{0-\frac{L}{2}}^{\frac{L}{2}} \tilde{w}(\phi, \nu) dx dy \\ &= 2 \frac{\Delta p L^6}{D_f} \int_{0-\frac{1}{2}}^1 \int_{0-\frac{1}{2}}^{\frac{1}{2}} \tilde{w}(\phi, \nu) d\tilde{x} d\tilde{y}. \end{aligned} \quad (16)$$

If we let the dimensionless integral equal $\tilde{V}(\phi, \nu)$, the change in volume is represented by

$$\Delta V = 2 \frac{\Delta p L^6}{D_f} \tilde{V}(\phi, \nu). \quad (17a)$$

Similar expressions can be developed for the two ϕ limits,

$$\Delta V = 2 \frac{\gamma_{vl} L^5}{D_f} \tilde{V}_s(\nu) \quad \phi \gg 1, \quad (17b)$$

$$\Delta V = 2 \frac{\Delta p L^6}{D_f} \tilde{V}_p(\nu) \quad \phi \ll 1, \quad (17c)$$

which are the result of integrating Eqs. (15b) and (15c), respectively.

The change in vapor/liquid interfacial area is found by integrating the displacement function along one of the deformed edges,

$$\begin{aligned} \Delta A_{vl} &= 4 \frac{\Delta p L^4}{D_f} \int_0^L \tilde{w}\left(x = \frac{L}{2}; \phi, \nu\right) dy \\ &= 4 \frac{\Delta p L^5}{D_f} \int_0^1 \tilde{w}\left(\tilde{x} = \frac{1}{2}; \phi, \nu\right) d\tilde{y}, \end{aligned} \quad (18)$$

where the “4” accounts for the four identical regions, one of which is indicated in the right panel of Figure 2. If we let the dimensionless integral equal $\tilde{A}(\phi, \nu)$, then the total change in vapor/liquid interfacial area is given by

$$\Delta A_{vl} = 4 \frac{\Delta p L^5}{D_f} \tilde{A}(\phi, \nu). \quad (19a)$$

In the two limits of ϕ we have

$$\Delta A_{vl} = 4 \frac{\gamma_{vl} L^4}{D_f} \tilde{A}_s(\nu) \quad \phi \gg 1, \quad (19b)$$

$$\Delta A_{vl} = 4 \frac{\Delta p L^5}{D_f} \tilde{A}_p(\nu) \quad \phi \ll 1. \quad (19c)$$

Accounting for both plates, the total strain energy is given by^{81,84} (see also Appendix A)

$$\begin{aligned} U_{strain} &= D_f \int_{0-\frac{L}{2}}^L \int_{0-\frac{L}{2}}^{\frac{L}{2}} \left\{ \left(\frac{\partial^2 w}{\partial x^2} + \frac{\partial^2 w}{\partial y^2} \right)^2 \right. \\ &\quad \left. + 2(1-\nu) \left[\left(\frac{\partial^2 w}{\partial x \partial y} \right)^2 - \frac{\partial^2 w}{\partial x^2} \frac{\partial^2 w}{\partial y^2} \right] \right\} dx dy, \end{aligned} \quad (20)$$

which can also be written as

$$\begin{aligned} U_{strain} &= \frac{\Delta p^2 L^6}{D_f} \int_{0-\frac{1}{2}}^1 \int_{0-\frac{1}{2}}^{\frac{1}{2}} [\tilde{w}_{\tilde{x}\tilde{x}}^2 + \tilde{w}_{\tilde{y}\tilde{y}}^2 + 2\nu \tilde{w}_{\tilde{x}\tilde{x}} \tilde{w}_{\tilde{y}\tilde{y}} \\ &\quad + 2(1-\nu) \tilde{w}_{\tilde{x}\tilde{y}}^2] d\tilde{x} d\tilde{y}, \end{aligned} \quad (21)$$

where \tilde{w}_{ij} denotes a second derivative with respect to i and j . If we let the dimensionless integral be represented by $\tilde{F}(\phi, \nu)$, we can develop a similar expression for the strain energy,

$$U_{strain} = \frac{\Delta p^2 L^6}{D_f} \tilde{F}(\phi, \nu). \quad (22a)$$

In the two limits of ϕ we have

$$U_{strain} = \frac{\gamma_{vl}^2 L^4}{D_f} \tilde{F}_s(\nu) \quad \phi \gg 1, \quad (22b)$$

$$U_{strain} = \frac{\Delta p^2 L^6}{D_f} \tilde{F}_p(\nu) \quad \phi \ll 1. \quad (22c)$$

C. Critical drying distance

Using the compact expressions presented above, we develop a relatively simple solution for the critical drying distance.

$$\begin{aligned} D_c &= -\frac{2\gamma_{vl} \cos \theta}{\Delta p [1 + \phi]} \\ &\quad + \frac{\Delta p L^4 [2\tilde{V}(\phi, \nu) + \phi \tilde{A}(\phi, \nu) - \tilde{F}(\phi, \nu)]}{D_f [1 + \phi]}. \end{aligned} \quad (23)$$

Using the relationship between the work done by the loads and the strain energy (see Appendix A), we can reduce this equation to

$$D_c = -\frac{2\gamma_{vl} \cos \theta}{\Delta p [1 + \phi]} + \frac{\Delta p L^4 [\tilde{V}(\phi, \nu) + \frac{\phi}{2} \tilde{A}(\phi, \nu)]}{D_f [1 + \phi]}. \quad (24)$$

TABLE I. Values needed to calculate the critical drying distance with Eqs. (25b) and (25c).

| ν | \tilde{V}_p | \tilde{A}_s |
|-------|---------------|---------------|
| 0.1 | 0.00837 | 0.0223 |
| 0.2 | 0.00850 | 0.0240 |
| 0.3 | 0.00873 | 0.0263 |
| 0.4 | 0.00913 | 0.0295 |
| 0.5 | 0.00978 | 0.0340 |

Using the definition of D_f [Eq. (10)] we obtain the equivalent expression,

$$D_c = -\frac{2\gamma_{vl} \cos \theta}{\Delta p [1 + \phi]} + \frac{12(1 - \nu^2)\Delta p L [\tilde{V}(\phi, \nu) + \frac{\phi}{2}\tilde{A}(\phi, \nu)]}{E\lambda^3 [1 + \phi]}, \quad (25a)$$

where the aspect ratio $\lambda = h/L$ has been introduced.

In the limit $\phi \ll 1$,

$$D_c = -\frac{2\gamma_{vl} \cos \theta}{\Delta p} + \frac{12(1 - \nu^2)\Delta p L}{E\lambda^3} \tilde{V}_p(\nu) \quad \phi \ll 1. \quad (25b)$$

In the limit $\phi \gg 1$,

$$D_c = -\frac{L \cos \theta}{2} + \frac{6(1 - \nu^2)\gamma_{vl}}{E\lambda^3} \tilde{A}_s(\nu) \quad \phi \gg 1. \quad (25c)$$

Thus, in the limits of large or small ϕ , we only need a single dimensionless deformation, provided in Table I as a function of Poisson's ratio, in addition to the system variables and material properties in order to calculate the critical drying distance. For intermediate values of ϕ , we need a value of $\tilde{V}(\phi, \nu) + \frac{\phi}{2}\tilde{A}(\phi, \nu)$, provided in Figure 4, to calculate the critical drying distance, using Eq. (25a). The range of intermediate values of ϕ , found to be roughly between 0.15 and 15, corresponds to when the flexible term in Eq. (25a) is within 10% of the flexible term of either Eq. (25b) or Eq. (25c).

IV. DISCUSSION

The critical drying distance between flexible materials [Eq. (8)] is the sum of the drying distance between perfectly rigid plates and a new term that accounts for flexibility. The above derivation [Eq. (25a)] allows us to compare how the rigid and flexible contributions to the overall drying distance

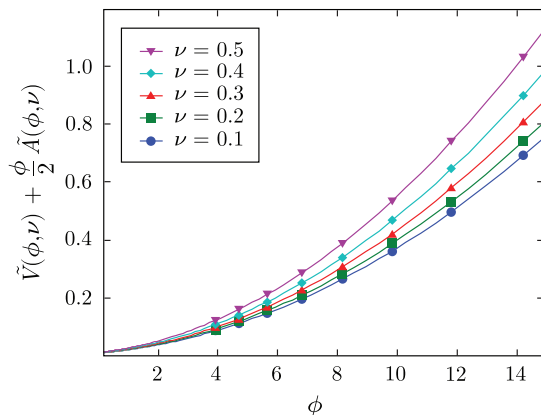


FIG. 4. For intermediate values of ϕ , the critical drying distance can be calculated using the information presented here along with Eq. (25a).

scale with material and environmental variables. For the purpose of this discussion we consider self-similar plates with $\lambda = 1/25$ at the large and small limits of ϕ . We also take the plates to be perfectly hydrophobic, meaning $\cos \theta = -1$. When $\phi \ll 1$, the rigid part of the solution behaves like a constant for a fixed T and μ of the surrounding bath, while the flexible term scales linearly with plate size. In $\phi \gg 1$ limit, the rigid part of the solution is on the order of the plate's size, while the flexible part behaves as a constant proportional to γ_{vl}/E . Thus, the scaling behavior of the rigid and flexible terms are switched at the two extremes of ϕ .

It is interesting to note that γ_{vl}/E is an important characteristic length scale in the study of elastocapillarity.⁸⁶⁻⁸⁸ In fact, an elastocapillary length proportional to γ_{vl}/E arises in the flexible term for both limits. To show this, we first make the numerical observation that in both limits,

$$12(1 - \nu^2)\tilde{V}_p(\nu) \approx 6(1 - \nu^2)\tilde{A}_s(\nu) \approx \frac{1}{10}, \quad (26)$$

which means we can approximate the flexible contributions as

$$D_{flex} \approx \frac{\Delta p L}{10E\lambda^3} \quad \phi \ll 1, \quad (27a)$$

$$D_{flex} \approx \frac{\gamma_{vl}}{10E\lambda^3} \quad \phi \gg 1. \quad (27b)$$

If we define D_{rigid} as the rigid contribution to the drying distance in the appropriate limit of ϕ one is considering, we can write the flexible contribution in the $\phi \ll 1$ limit as

$$D_{flex} \approx \frac{\Delta p}{2\gamma_{vl}} \frac{\gamma_{vl}}{5E\lambda^3} L = \frac{L_{EC}}{D_{rigid}} L \quad \phi \ll 1, \quad (28a)$$

where the elastocapillary length L_{EC} has been defined as $\frac{\gamma_{vl}}{5E\lambda^3}$. The term λ^3 is certainly an important component of the characteristic deformation, and the numerical prefactor has been included for convenience. The $\phi \gg 1$ limit is given by

$$D_{flex} \approx \frac{L_{EC}}{2} \quad \phi \gg 1. \quad (28b)$$

It can be seen from Eqs. (28a) and (28b) that the flexible contributions behave rather differently with respect to characteristic size in the two limits.

The opposite scaling behavior with respect to plate size between the flexible and rigid contributions to the drying distance, alluded to above, becomes more apparent if we consider their ratio. In the small ϕ limit, this ratio is given by

$$\frac{D_{flex}}{D_{rigid}} \approx \frac{L_{EC}}{D_{rigid}^2} L \quad \phi \ll 1, \quad (29a)$$

while in the large ϕ limit it is given by

$$\frac{D_{flex}}{D_{rigid}} \approx \frac{L_{EC}}{L} \quad \phi \gg 1. \quad (29b)$$

The former scales with L whereas the latter scales with $1/L$.

For flexibility to be important to the thermodynamics of drying, the quantity D_{flex} must be comparable to D_{rigid} . This can easily be assessed through the ratios provided in Eqs. (29a) and (29b). Since ϕ depends on both the characteristic size and thermodynamic conditions, we narrow this discussion by considering three state points for water detailed

TABLE II. Lower and upper bound on plate size needed for ϕ to be small (≤ 0.15) or large (≥ 15), respectively, at three water state points.

| State point ^a | $\phi \ll 1$ | | $\phi \gg 1$ | |
|--------------------------|------------------|------------------|----------------|---------------------------|
| | L_{min} | D_{rigid} (nm) | L_{max} (nm) | $D_{rigid}(L_{max})$ (nm) |
| 20 °C 1 bar | 20 μm | 1440 | 200 | 100 |
| 90 °C 1 bar | 70 μm | 4670 | 700 | 350 |
| 20 °C 2 kbar | 10 nm | 0.72 | 0.1 | 0.05 |

^aWhen ϕ is small, the rigid contribution to the drying distance is constant at a given state point. When ϕ is large, the rigid solution is dependent on the characteristic size, which therefore places a maximum bound on the rigid contribution.

in Table II. Picking a state point puts a lower bound on the characteristic size needed for ϕ to be small ($\phi \leq 0.15$) and an upper bound on the characteristic size needed for ϕ to be large ($\phi \geq 15$) (provided in Table II). As an example we consider two representative materials: amyloid fibrils ($E \sim 1$ GPa) and glass ($E \sim 100$ GPa).⁸⁹ While typical glass is not the perfectly hydrophobic material ($\theta = 180^\circ$) that was introduced at the outset of this discussion, we call this material glass primarily to provide the reader with some physical intuition regarding its stiffness. In addition, a number of experiments studying the forces between hydrophobic surfaces are conducted using surface-modified glass as the confining material.⁹⁰

Figure 5 presents the ratio of the flexible to the rigid contribution at a given state point, plotted against the rigid contribution, for $\phi \ll 1$. The L used in calculating these ratios is L_{min} from Table II, so these ratios represent a lower bound. At moderate pressures, the drying distance for the amyloid material is the result of comparable rigid and flexible contributions, while for glass, the flexible contribution is negligible. At elevated pressures, the flexible contribution is the dominant component to the drying distance for either material. At such high pressures, some caution is warranted, as we are pushing the assumption of small deformations. Nonetheless, the present analysis suggests that while D_{rigid} is suppressed at

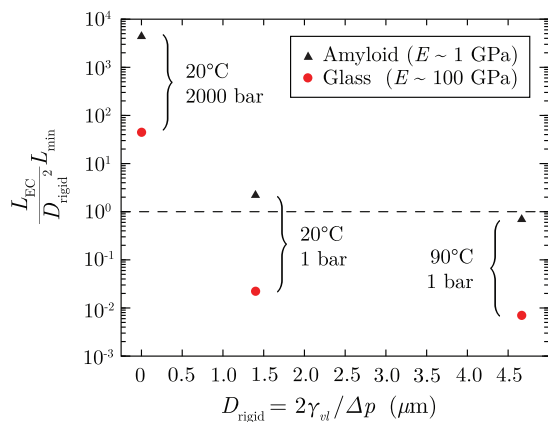


FIG. 5. The ratio between the flexible and rigid contributions to the drying distance against the rigid solution for $\phi \ll 1$ is shown at three water state points for two materials. Both materials in this example have a characteristic size of L_{min} , which is the minimum size required to be within the $\phi \ll 1$ limit. Since the ratio shown on the y-axis scales by L , the values presented represent a lower bound. Values above the dashed line, indicating unity, correspond to cases where the flexible contribution to the drying distance is greater than the rigid contribution.

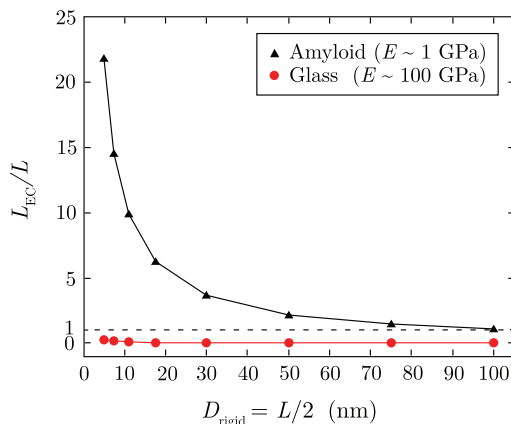


FIG. 6. The ratio between the flexible and rigid contributions to the drying distance for water at ambient conditions, as a function the rigid contribution for $\phi \gg 1$. This ratio decays like $1/L$, and the elastocapillary length L_{EC} alone determines the overall ratio for a given characteristic size.

elevated pressure, a prediction consistent with simulations of rigid solutes,^{13,44} the flexible contribution is capable of compensating for a significant portion of this pressure-induced reduction, resulting in an overall drying distance that can remain roughly constant or even grow with pressure.

Figure 6 shows the ratio of the flexible to the rigid contribution at moderate pressure, plotted against the rigid contribution, for $\phi \gg 1$. At elevated pressures, $\phi \gg 1$ requires L to be very small, on the order of a few angstroms (see Table II), so we confine our attention of the large ϕ limit to moderate pressures. For the amyloid, the flexible contribution remains dominant until the characteristic length is $\mathcal{O}(100$ nm). This suggests that for small and relatively soft materials at ambient conditions, the overall drying distance would appear to be relatively constant, rather than scaling with characteristic size of the hydrophobic object. For glass, however, the rigid solution is always the dominant contribution to the drying distance, so one would expect the drying distance to scale with size.

We conclude this discussion by considering how the trends noted above may inform the rational design of hydrophobic assemblies. Given the opposite scaling behavior of the rigid and flexible terms at the small and large ϕ limits, considering flexibility as a design parameter may allow more versatility in the engineering of hydrophobic assemblies. For nanoscale assemblies at ambient conditions (i.e., the $\phi \gg 1$ limit), the rigid solution suggests that one is limited to tuning size (L) and to some degree chemistry (θ). By accounting for flexibility, we see that the mechanical properties (E) and shape (λ) can be important design parameters. For micron-sized assemblies at ambient conditions (i.e., the $\phi \ll 1$ limit), flexibility introduces size, shape, and mechanical properties as design variables. In addition, flexibility may be an important part of understanding the behavior of assemblies at extreme conditions, such as elevated pressure.

V. CONCLUSION

In this work, we have developed a thermodynamic theory of drying between flexible materials by determining the critical drying distance of a liquid confined between linear elastic plate-like solutes. The resulting expression for the critical

drying distance is the sum of the drying distance between perfectly rigid plates and a new term that accounts for flexibility. The energetic penalties of drying, the reduction in bulk fluid free energy and formation of a vapor/liquid interface, result in forces acting on the plates upon drying. Allowing plate flexibility relieves these penalties to some extent, but at the cost of introducing strain in the plates. However, thermodynamic arguments show that the free energy decrease associated with this relief outweighs the free energy increase associated with strain. Thus, the term accounting for flexibility is necessarily positive, meaning that flexibility augments the critical drying distance.

In order to estimate the magnitude of the flexible term's contribution to the critical drying distance and investigate the expected scaling behavior, we considered the example of drying between plates that are simply supported at two edges and free at the remaining ones. This analysis yielded a relatively simple expression for the drying distance that behaves differently depending on the relative weights of the energetic penalties to drying, quantified through the dimensionless group ϕ . At the large and small limits of this dimensionless group, the scaling behavior of the two terms in the expression for the drying distance are quite different, suggesting that considering flexibility broadens the ability to design hydrophobic assemblies at various length scales. By comparing the ratios of the rigid and flexible contributions to the overall drying distance, we showed that for water at ambient conditions, at least half of the drying distance can come from the flexible term for materials with a Young's modulus of the order of 1 GPa (e.g., amyloid fibrils). For objects with a sufficiently small characteristic size, roughly 10 nm in our example, the flexible term is the dominant contribution to the overall drying distance. At elevated pressures, materials with moduli as large as 100 GPa (e.g., glass) are expected to have drying distances well approximated by the flexible term.

Given the number of simplifying assumptions invoked in our analysis, there exist numerous avenues worth exploring to enrich the ideas presented here. We have considered the existence of only two stable states: a completely wet and a completely dry confined region. It would be interesting to investigate whether flexibility introduces additional free energy minima associated with incomplete drying. In addition, while we have introduced a feature of 'real' materials (i.e., flexibility) into the problem of hydrophobic drying, our system is still highly idealized. Assessing how flexibility mediates the behavior of assemblies such as membrane channels or protein-ligand complexes is an interesting problem. While we have addressed the purely thermodynamic question of when drying between flexible substrates becomes favorable, exploring how flexibility affects the kinetics of drying is another important problem whose solution could yield fresh insights into the design of hydrophobic assemblies. This last question regarding kinetics is one that we are currently exploring via molecular simulations.

ACKNOWLEDGMENTS

Y.E.A. is grateful to Jonathan Glassman and Howard Stone for helpful discussions and Nyssa Emerson for figure

preparation assistance. P.G.D. gratefully acknowledges the support of the National Science Foundation (Grant No. CHE-1213343).

APPENDIX A: THERMODYNAMICS OF AN ELASTIC SOLID

The differential form of the fundamental equation for a volume element of an elastic solid subject to small deformations is given by

$$d\underline{U} = Td\underline{S} + \sigma_{ij}d\epsilon_{ij}, \quad (\text{A1})$$

where σ_{ij} and ϵ_{ij} are components of the stress tensor σ and strain tensor ϵ , and \underline{U} is the internal energy and \underline{S} is the entropy, both in volume intensive units.⁸¹ Since we are interested in the behavior of a flexible solid in contact with a constant temperature reservoir (the bulk fluid), the canonical thermodynamic variables are the solid's temperature and state of strain. This means that the Helmholtz free energy is the appropriate potential for the solid, whose differential form is obtained through the first Legendre transform of the fundamental equation,

$$d\underline{A} = -\underline{S}dT + \sigma_{ij}d\epsilon_{ij}. \quad (\text{A2})$$

If the solid undergoes an isothermal change in its state of strain, the differential can be integrated to yield,

$$\underline{A} = \underline{A}_0(T) + \int_0^{\epsilon_{ij}} \sigma_{ij}d\epsilon'_{ij} = \underline{A}_0(T) + \underline{U}_{strain}, \quad (\text{A3})$$

where $\underline{A}_0(T)$ is some function of temperature and the integral over the components of strain is the strain energy per unit volume. Given the form above, one can describe an isothermal change in strain solely through the strain energy.

Limiting the analysis to an isotropic linear elastic (Hookean) solid, the strain energy is given by a quadratic function of the strain components.⁸¹ Since the strain energy is a quadratic function of strain, one can apply Euler's theorem for homogeneous functions to show that

$$2\underline{A} = \epsilon_{ij} \left(\frac{\partial \underline{A}}{\partial \epsilon_{ij}} \right)_T = \sigma_{ij}\epsilon_{ij}. \quad (\text{A4})$$

Since $\sigma_{ij}\epsilon_{ij}$ is the work per unit volume performed by the stress σ_{ij} deforming solid element, we see that the free energy change of the solid strained isothermally will be half the work performed on that element.

For a thin elastic plate, the strain energy of a single plate can be independently calculated through

$$F = \frac{1}{2}D_f \iint \left\{ \left(\frac{\partial^2 w}{\partial x^2} + \frac{\partial^2 w}{\partial y^2} \right)^2 + 2(1-\nu) \left[\left(\frac{\partial^2 w}{\partial x \partial y} \right)^2 - \frac{\partial^2 w}{\partial x^2} \frac{\partial^2 w}{\partial y^2} \right] \right\} dx dy, \quad (\text{A5})$$

where w is the deflection profile of the plate and the integral is over the entire domain of the plate.⁸¹

APPENDIX B: DEVELOPMENT OF $w(x, y)$

Here, we provide a more detailed derivation of the deflection profile for a plate simply supported at edges $y = 0, L$ and free at the edges $x = -\frac{L}{2}, \frac{L}{2}$ (Figure 3), subject to a uniform load Δp and an effective shear force at the free edges γ_{vl} , both oriented in the positive z -direction. We use the series solution suggested by Lévy,⁸⁴

$$w = w_1 + w_2,$$

$$w_1 = \frac{\Delta p L^4}{D_f} \sum_{m=1,3,5,\dots}^{\infty} \frac{4}{(m\pi)^5} \sin\left(\frac{m\pi y}{L}\right),$$

$$w_2 = \sum_{m=1,3,5,\dots}^{\infty} Y_m(x) \sin\left(\frac{m\pi y}{L}\right), \quad (\text{B1})$$

$$Y_m(x) = \frac{\Delta p L^4}{D_f} \left[A_m \cosh\left(\frac{m\pi x}{L}\right) + B_m \frac{m\pi x}{L} \sinh\left(\frac{m\pi x}{L}\right) + C_m \sinh\left(\frac{m\pi x}{L}\right) + D_m \frac{m\pi x}{L} \cosh\left(\frac{m\pi x}{L}\right) \right],$$

where $A_m, B_m, C_m,$ and D_m are coefficients that are unique to a particular set of boundary conditions. Due to symmetry across the y -axis, only even expressions in $Y_m(x)$ should be retained,

$$Y_m(x) = \frac{\Delta p L^4}{D_f} \left[A_m \cosh\left(\frac{m\pi x}{L}\right) + B_m \frac{m\pi x}{L} \sinh\left(\frac{m\pi x}{L}\right) \right], \quad (\text{B2})$$

meaning $C_m = D_m = 0$.

The boundary conditions at the simply supported edges $y = 0, L$ are

$$w = 0 \quad \frac{\partial^2 w}{\partial y^2} = 0, \quad (\text{B3})$$

which are both already satisfied. The boundary conditions at edges $x = -\frac{L}{2}, \frac{L}{2}$ are

$$\frac{\partial^2 w}{\partial x^2} + \nu \frac{\partial^2 w}{\partial y^2} = 0 \quad (\text{B4})$$

and

$$-D_f \left(\frac{\partial^3 w}{\partial x^3} + (2 - \nu) \frac{\partial^3 w}{\partial x \partial y^2} \right) = \gamma_{vl}. \quad (\text{B5})$$

We can find the desired coefficients by expressing boundary conditions in terms of derivatives of the above equation. If we let $\alpha_m = \frac{m\pi}{2}$, then boundary condition given in Eq. (B4) yields,

$$\sum_{m=1,3,5,\dots}^{\infty} \left[A_m (1 - \nu) \cosh \alpha_m + B_m [2 \cosh \alpha_m + (1 - \nu) \alpha_m \sinh \alpha_m] - \frac{4\nu}{(m\pi)^5} \right] = 0. \quad (\text{B6})$$

Since this can be satisfied by setting inside of the summation equal to zero for any m , the first boundary condition becomes.

$$A_m (1 - \nu) \cosh \alpha_m + B_m [2 \cosh \alpha_m + (1 - \nu) \alpha_m \sinh \alpha_m] = \frac{4\nu}{(m\pi)^5}. \quad (\text{B7})$$

In order to proceed with the second boundary condition [Eq. (B5)], we set the constant γ_{vl} equal to its Fourier sine series on the interval $y \in (0, L)$,

$$\gamma_{vl} = \sum_{m=1,3,5,\dots}^{\infty} \frac{4\gamma_{vl}}{m\pi} \sin\left(\frac{m\pi y}{L}\right). \quad (\text{B8})$$

The boundary condition now becomes

$$-\Delta p L \sum_{m=1,3,5,\dots}^{\infty} \left(\frac{m\pi}{L}\right)^3 \{A_m (\nu - 1) \sinh \alpha_m + B_m [(1 + \nu) \sinh \alpha_m + (\nu - 1) \alpha_m \cosh \alpha_m]\} \sin\left(\frac{m\pi y}{L}\right) = \sum_{m=1,3,5,\dots}^{\infty} \frac{4\gamma_{vl}}{m\pi} \sin\left(\frac{m\pi y}{L}\right), \quad (\text{B9})$$

which simplifies to

$$A_m (\nu - 1) \sinh \alpha_m + B_m [(1 + \nu) \sinh \alpha_m + (\nu - 1) \alpha_m \cosh \alpha_m] = -\frac{\phi}{(m\pi)^4}. \quad (\text{B10})$$

Solving for A_m and B_m yields,

$$A_m = \frac{4}{(m\pi)^5} \frac{\nu (1 + \nu) \sinh \alpha_m - \nu (1 - \nu) \alpha_m \cosh \alpha_m + \left(\frac{m\pi\phi}{4}\right) [2 \cosh \alpha_m + (1 - \nu) \alpha_m \sinh \alpha_m]}{(3 + \nu) (1 - \nu) \sinh \alpha_m \cosh \alpha_m - (1 - \nu)^2 \alpha_m}, \quad (\text{B11})$$

$$B_m = \frac{4}{(m\pi)^5} \frac{\nu(1-\nu) \sinh \alpha_m - \left(\frac{m\pi\phi}{4}\right) (1-\nu) \cosh \alpha_m}{(3+\nu)(1-\nu) \sinh \alpha_m \cosh \alpha_m - (1-\nu)^2 \alpha_m}. \quad (\text{B12})$$

The accompanying series solution is

$$w(x, y) = \frac{\Delta p L^4}{D_f} \sum_{m=1,3,5,\dots}^{\infty} \left[\frac{4}{(m\pi)^5} + A_m \cosh\left(\frac{m\pi x}{L}\right) + B_m \frac{m\pi x}{L} \sinh\left(\frac{m\pi x}{L}\right) \right] \sin\left(\frac{m\pi y}{L}\right). \quad (\text{B13})$$

If we let

$$\tilde{w}(\phi, \nu) = \sum_{m=1,3,5,\dots}^{\infty} \left[\frac{4}{(m\pi)^5} + A_m \cosh(m\pi \tilde{x}) + B_m m\pi \tilde{x} \sinh(m\pi \tilde{x}) \right] \sin(m\pi \tilde{y}), \quad (\text{B14})$$

then the solution can be written as

$$w(x, y) = \frac{\Delta p L^4}{D_f} \tilde{w}(\phi, \nu). \quad (\text{B15})$$

We can obtain the limits of the deformation function for large and small ϕ . In the large ϕ limit, the deflection is described by

$$w(x, y) = \frac{\gamma_{vl} L^3}{D_f} \sum_{m=1,3,5,\dots}^{\infty} \left[A'_m \cosh\left(\frac{m\pi x}{L}\right) + B'_m \frac{m\pi x}{L} \sinh\left(\frac{m\pi x}{L}\right) \right] \sin\left(\frac{m\pi y}{L}\right), \quad (\text{B16})$$

$$A'_m = \frac{4}{(m\pi)^4} \frac{2 \cosh \alpha_m + (1-\nu) \alpha_m \sinh \alpha_m}{(3+\nu)(1-\nu) \sinh \alpha_m \cosh \alpha_m - (1-\nu)^2 \alpha_m}, \quad (\text{B17})$$

$$B'_m = \frac{4}{(m\pi)^4} \frac{-(1-\nu) \cosh \alpha_m}{(3+\nu)(1-\nu) \sinh \alpha_m \cosh \alpha_m - (1-\nu)^2 \alpha_m}. \quad (\text{B18})$$

If we let

$$\tilde{w}_s(\nu) = \sum_{m=1,3,5,\dots}^{\infty} [A'_m \cosh(m\pi \tilde{x}) + B'_m m\pi \tilde{y} \sinh(m\pi \tilde{x})] \sin(m\pi \tilde{y}), \quad (\text{B19})$$

then the solution in this limit can be written as

$$w(x, y) = \frac{\gamma_{vl} L^3}{D_f} \tilde{w}_s(\nu) \quad \phi \gg 1. \quad (\text{B20})$$

In the small ϕ limit, the deflection is described by

$$w(x, y) = \frac{\Delta p L^4}{D_f} \sum_{m=1,3,5,\dots}^{\infty} \left[\frac{4}{(m\pi)^5} + A''_m \cosh\left(\frac{m\pi x}{L}\right) + B''_m \frac{m\pi x}{L} \sinh\left(\frac{m\pi x}{L}\right) \right] \sin\left(\frac{m\pi y}{L}\right), \quad (\text{B21})$$

$$A''_m = \frac{4}{(m\pi)^5} \frac{\nu(1+\nu) \sinh \alpha_m - \nu(1-\nu) \alpha_m \cosh \alpha_m}{(3+\nu)(1-\nu) \sinh \alpha_m \cosh \alpha_m - (1-\nu)^2 \alpha_m}, \quad (\text{B22})$$

$$B''_m = \frac{4}{(m\pi)^5} \frac{\nu(1-\nu) \sinh \alpha_m}{(3+\nu)(1-\nu) \sinh \alpha_m \cosh \alpha_m - (1-\nu)^2 \alpha_m}. \quad (\text{B23})$$

If we let

$$\tilde{w}_p(\nu) = \sum_{m=1,3,5,\dots}^{\infty} \left[\frac{4}{(m\pi)^5} + A''_m \cosh(m\pi \tilde{x}) + B''_m m\pi \tilde{x} \sinh(m\pi \tilde{x}) \right] \sin(m\pi \tilde{y}), \quad (\text{B24})$$

then the solution in this limit can be written as

$$w(x, y) = \frac{\Delta p L^4}{D_f} \tilde{w}_p(\nu) \quad \phi \ll 1. \quad (\text{B25})$$

¹J. S. Rowlinson and B. Widom, *Molecular Theory of Capillarity* (Dover, Mineola, 1982).

²P. Ball, *Chem. Rev.* **108**, 74 (2008).

³P. G. Debenedetti, *J. Phys.: Condens. Matter* **15**, R1669 (2003).

⁴F. H. Stillinger, *Science* **209**, 451 (1980).

⁵T. B. Sisan and S. Lichter, *Phys. Rev. Lett.* **112**, 044501 (2014).

⁶A. Fallah-Araghi *et al.*, *Phys. Rev. Lett.* **112**, 028301 (2014).

⁷A. Siria *et al.*, *Nature (London)* **494**, 455 (2013).

⁸M. A. Shannon *et al.*, *Nature (London)* **452**, 301 (2008).

⁹R. D. Piner *et al.*, *Science* **283**, 661 (1999).

¹⁰K. Jo *et al.*, *Proc. Natl. Acad. Sci. U.S.A.* **104**, 2673 (2007).

¹¹J. C. Rasaiah, S. Garde, and G. Hummer, *Annu. Rev. Phys. Chem.* **59**, 713 (2008).

¹²B. J. Berne, J. D. Weeks, and R. H. Zhou, *Annu. Rev. Phys. Chem.* **60**, 85 (2009).

¹³N. Giovambattista, P. J. Rossky, and P. G. Debenedetti, *Annu. Rev. Phys. Chem.* **63**, 179 (2012).

¹⁴M. F. Emerson and A. Holtzer, *J. Phys. Chem.* **71**, 3320 (1967).

¹⁵L. Maibaum, A. R. Dinner, and D. Chandler, *J. Phys. Chem. B* **108**, 6778 (2004).

¹⁶C. Tanford, *J. Am. Chem. Soc.* **84**, 4240 (1962).

¹⁷W. C. Wimley and S. H. White, *Biochemistry* **32**, 6307 (1993).

¹⁸A. Anishkin and S. Sukharev, *Biophys. J.* **86**, 2883 (2004).

¹⁹F. Q. Zhu and G. Hummer, *Proc. Natl. Acad. Sci. U.S.A.* **107**, 19814 (2010).

²⁰M. O. Jensen *et al.*, *Proc. Natl. Acad. Sci. U.S.A.* **107**, 5833 (2010).

²¹W. Kauzmann, *Adv. Protein Chem.* **14**, 1 (1959).

²²K. A. Dill, *Biochemistry* **29**, 7133 (1990).

²³D. Chandler, *Nature (London)* **437**, 640 (2005).

²⁴R. A. Pierotti, *J. Phys. Chem.* **69**, 281 (1965).

²⁵L. R. Pratt and D. Chandler, *J. Chem. Phys.* **67**, 3683 (1977).

²⁶S. Garde *et al.*, *Phys. Rev. Lett.* **77**, 4966 (1996).

²⁷G. Hummer *et al.*, *Proc. Natl. Acad. Sci. U.S.A.* **93**, 8951 (1996).

²⁸G. Hummer *et al.*, *J. Phys. Chem. B* **102**, 10469 (1998).

²⁹F. H. Stillinger, *J. Solution Chem.* **2**, 141 (1973).

³⁰C. Y. Lee, J. A. McCammon, and P. J. Rossky, *J. Chem. Phys.* **80**, 4448 (1984).

³¹K. Lum, D. Chandler, and J. D. Weeks, *J. Phys. Chem. B* **103**, 4570 (1999).

³²S. Rajamani, T. M. Truskett, and S. Garde, *Proc. Natl. Acad. Sci. U.S.A.* **102**, 9475 (2005).

³³H. S. Ashbaugh and L. R. Pratt, *Rev. Mod. Phys.* **78**, 159 (2006).

³⁴A. Geiger, A. Rahman, and F. H. Stillinger, *J. Chem. Phys.* **70**, 263 (1979).

³⁵C. Pangali, M. Rao, and B. J. Berne, *J. Chem. Phys.* **71**, 2982 (1979).

³⁶K. Watanabe and H. C. Andersen, *J. Phys. Chem.* **90**, 795 (1986).

³⁷A. Wallqvist and B. J. Berne, *J. Phys. Chem.* **99**, 2893 (1995).

³⁸K. Lum and A. Luzar, *Phys. Rev. E* **56**, R6283 (1997).

- ³⁹A. Luzar and K. Leung, *J. Chem. Phys.* **113**, 5836 (2000).
- ⁴⁰K. Leung and A. Luzar, *J. Chem. Phys.* **113**, 5845 (2000).
- ⁴¹K. Leung, A. Luzar, and D. Bratko, *Phys. Rev. Lett.* **90**, 065502 (2003).
- ⁴²A. Luzar, *J. Phys. Chem. B* **108**, 19859 (2004).
- ⁴³X. Huang, C. J. Margulis, and B. J. Berne, *Proc. Natl. Acad. Sci. U.S.A.* **100**, 11953 (2003).
- ⁴⁴N. Giovambattista, P. J. Rossky, and P. G. Debenedetti, *Phys. Rev. E* **73**, 041604 (2006).
- ⁴⁵S. Sharma and P. G. Debenedetti, *Proc. Natl. Acad. Sci. U.S.A.* **109**, 4365 (2012).
- ⁴⁶S. Sharma and P. G. Debenedetti, *J. Phys. Chem. B* **116**, 13282 (2012).
- ⁴⁷A. L. Ferguson *et al.*, *J. Chem. Phys.* **137**, 144501 (2012).
- ⁴⁸J. Y. Li, J. A. Morrone, and B. J. Berne, *J. Phys. Chem. B* **116**, 11537 (2012).
- ⁴⁹J. A. Morrone, J. Li, and B. J. Berne, *J. Phys. Chem. B* **116**, 378 (2012).
- ⁵⁰P. Liu *et al.*, *Nature (London)* **437**, 159 (2005).
- ⁵¹F. Q. Zhu and G. Hummer, *Biophys. J.* **103**, 219 (2012).
- ⁵²R. O. Dror *et al.*, *Proc. Natl. Acad. Sci. U.S.A.* **108**, 13118 (2011).
- ⁵³N. Giovambattista *et al.*, *Proc. Natl. Acad. Sci. U.S.A.* **105**, 2274 (2008).
- ⁵⁴T. Young *et al.*, *Proteins: Struct., Funct., Bioinf.* **78**, 1856 (2010).
- ⁵⁵H. K. Christenson and P. M. Claesson, *Science* **239**, 390 (1988).
- ⁵⁶J. L. Parker, P. M. Claesson, and P. Attard, *J. Phys. Chem.* **98**, 8468 (1994).
- ⁵⁷P. M. Claesson and H. K. Christenson, *J. Phys. Chem.* **92**, 1650 (1988).
- ⁵⁸V. V. Yaminsky *et al.*, *J. Colloid Interface Sci.* **96**, 301 (1983).
- ⁵⁹V. S. Yushchenko, V. V. Yaminsky, and E. D. Shchukin, *J. Colloid Interface Sci.* **96**, 307 (1983).
- ⁶⁰Y. I. Rabinovich, B. V. Derjaguin, and N. V. Churaev, *Adv. Colloid Interface Sci.* **16**, 63 (1982).
- ⁶¹C. A. Cerdeirina *et al.*, *J. Phys. Chem. Lett.* **2**, 1000 (2011).
- ⁶²T. Young, *Philos. Trans. R. Soc. London* **95**, 65 (1805).
- ⁶³G. R. Lester, *J. Colloid Sci.* **16**, 315 (1961).
- ⁶⁴E. R. Jerison *et al.*, *Phys. Rev. Lett.* **106**, 186103 (2011).
- ⁶⁵Y. S. Yu, *Appl. Math. Mech.* **33**, 1095 (2012).
- ⁶⁶L. M. Xu and V. Molinero, *J. Phys. Chem. B* **114**, 7320 (2010).
- ⁶⁷H. S. Ashbaugh, *J. Chem. Phys.* **139**, 064702 (2013).
- ⁶⁸A. Luzar, D. Bratko, and L. Blum, *J. Chem. Phys.* **86**, 2955 (1987).
- ⁶⁹A. P. Willard and D. Chandler, *Faraday Discuss.* **141**, 209 (2009).
- ⁷⁰H. Acharya *et al.*, *Faraday Discuss.* **146**, 353 (2010).
- ⁷¹T. Koishi *et al.*, *J. Chem. Phys.* **123**, 204707 (2005).
- ⁷²N. Giovambattista, P. G. Debenedetti, and P. J. Rossky, *J. Phys. Chem. C* **111**, 1323 (2007).
- ⁷³N. Giovambattista, P. J. Rossky, and P. G. Debenedetti, *J. Phys. Chem. B* **113**, 13723 (2009).
- ⁷⁴L. Hua, R. Zangi, and B. J. Berne, *J. Phys. Chem. C* **113**, 5244 (2009).
- ⁷⁵Y. K. Cheng and P. J. Rossky, *Nature (London)* **392**, 696 (1998).
- ⁷⁶J. Mittal and G. Hummer, *Faraday Discuss.* **146**, 341 (2010).
- ⁷⁷S. Singh *et al.*, *Nature (London)* **442**, 526 (2006).
- ⁷⁸O. Beckstein and M. S. P. Sansom, *Phys. Biol.* **1**, 42 (2004).
- ⁷⁹S. Andreev, D. R. Reichman, and G. Hummer, *J. Chem. Phys.* **123**, 194502 (2005).
- ⁸⁰G. Hummer, J. C. Rasaiah, and J. P. Noworyta, *Nature (London)* **414**, 188 (2001).
- ⁸¹L. D. Landau and E. M. Lifshitz, *Theory of Elasticity* (Pergamon, Oxford, 1986).
- ⁸²A. E. H. Love, *A Treatise on the Mathematical Theory of Elasticity*, 4th ed. (Dover, New York, 1944).
- ⁸³J. H. Wang *et al.*, *Phys. Chem. Chem. Phys.* **13**, 19902 (2011).
- ⁸⁴S. Timoshenko and S. Woinowsky-Krieger, *Theory of Plates and Shells*, 2nd ed. (McGraw-Hill, New York, 1968).
- ⁸⁵G. T. Lim and J. N. Reddy, *Int. J. Solids Struct.* **40**, 3039 (2003).
- ⁸⁶B. Roman and J. Bico, *J. Phys.: Condens. Matter* **22**, 493101 (2010).
- ⁸⁷A. Marchand *et al.*, *Phys. Rev. Lett.* **109**, 236101 (2012).
- ⁸⁸J. S. Wexler, T. M. Heard, and H. A. Stone, *Phys. Rev. Lett.* **112**, 066102 (2014).
- ⁸⁹T. P. J. Knowles and M. J. Buehler, *Nat. Nanotechnol.* **6**, 469 (2011).
- ⁹⁰H. K. Christenson and P. M. Claesson, *Adv. Colloid Interface Sci.* **91**, 391 (2001).